CARBON 46 (2008) 741–746

available at www.sciencedirect.com

ScienceDirect

journal homepage: www.elsevier.com/locate/carbon

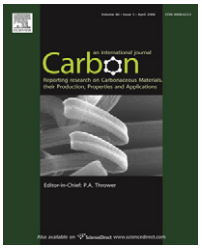

Quasi two-dimensional carbon nanobelts synthesized using a template method

Cheng-Te Lin[a], *Tsung-Han Chen*[a], *Tsung-Shune Chin*[b], *Chi-Young Lee*[a,c,*], *Hsin-Tien Chiu*[d]

[a]*Department of Materials Science and Engineering, National Tsing Hua University, Hsinchu 30013, Taiwan*
[b]*Department of Materials Science and Engineering, Feng-Chia University, Taichung 40724, Taiwan*
[c]*Center of Nanotechnology, Materials Science and Microsystems, National Tsing Hua University, Hsinchu 30013, Taiwan*
[d]*Department of Applied Chemistry, National Chiao Tung University, Hsinchu 30050, Taiwan*

ARTICLE INFO

Article history:
Received 17 August 2007
Accepted 26 January 2008
Available online 8 February 2008

ABSTRACT

Carbon nanobelts have been synthesized using nanoporous anodic alumina as template and ethanol as precursor. The length and width are tens of micrometers and 470 nm, respectively. The thickness was measured to be 5 nm, exhibiting a high-aspect-ratio morphology. After annealing, the crystallinity of the nanobelts can be improved. The formation mechanism of such morphology is demonstrated as a radial deformation of large thin nanotubes. This is disclosed for the first time in the literature regarding the attainment of a quasi two-dimensional nanocarbon via a template route. Field emission measurements on the sample annealed at 800 °C show a turn-on voltage 3.25 V/μm and stable long-term emission efficiency. The lower threshold voltage is attributed to the strong edge emitter effect.

1. Introduction

Template-mediated growth method is always worth being considered as scientists intend to produce a nano-sized material. Although the indispensable etching process for removal of the nanoporous oxide template restricts its applications, template method still possesses many non-substitutable advantages, such as uniform sample sizes, self-alignment, catalyst-free, and morphology controllability. Therefore, now this method has been a world-widely adopted technique to synthesize nanocarbons in zero to three dimensions and makes a significant progress in last ten years [1–3]. Various carbon materials, like nanoparticles [1,4], nanotubes [5,6], nanofilaments [7,8], ultra-thin graphite films [9,10] and ordered micro- or meso-porous carbons [3,11] have been successfully obtained using different kinds of templates. However, quasi two-dimensional (quasi-2D) products are absent from the groups as above mentioned. The quasi-2D materials are usually composed of finitely superficial size or exhibit two-dimensional large-aspect-ratio, and their thickness is extremely thin to be more than one order of magnitude smaller than length and width. The current quasi-2D nanocarbons, like nanowalls, nanosheets, and nanobelts, are synthesized by the hydrothermal method [12] or plasma-enhanced chemical vapor deposition (PECVD) [13,14]. Further electronic investigation demonstrated that the quasi-2D carbons nanomaterials reveal excellent field emission characteristics [13], and their strip morphology may have a potential application as the electron-transport carrier.

In this study, a massive amount of belt-like carbon materials was obtained using a nanoporous template. The products

* *Corresponding author.* Address: Department of Materials Science and Engineering, National Tsing Hua University, 101, Section 2, Kuang-Fu Road, Hsinchu 30013, Taiwan. Fax: +886 3 5166687.
E-mail address: cylee@mx.nthu.edu.tw (C.-Y. Lee).
0008-6223/$ - see front matter © 2008 Elsevier Ltd. All rights reserved.
doi:10.1016/j.carbon.2008.01.034

with high-aspect-ratios agree with the definition of quasi-2D material. Such a distinctive structure which has never been found with a similar method is disclosed herewith. The appearance, microstructure, and formation mechanism of the belt-like morphology are characterized and discussed. The effect on crystallinity of thermal treatment, and the field emitting properties under optimized conditions are further studied as well.

2. Experimental

Fig. 1 illustrates the experimental procedures. The products were synthesized by APCVD using dehydrated ethanol as precursor and anodic aluminum oxide as templates. Both commercial (Whatman Ltd.) and home made porous alumina were used as templates. The home made templates were produced by using the conventional anodization procedures [15]. The APCVD system consists of a tube furnace and a pumping system. The tube furnace was pre-heated to 550 °C with Ar flow 30 sccm. After inserting templates, Ar gas was used to carry the dehydrated ethanol and introduce the vaporized ethanol into the system. Then the vaporized ethanol would be decomposed at 550 °C and coat on the channel surface of the templates. After reaction for 90 min, the templates retrieved from the tube furnace became totally black. The templates were then removed by immersing in sodium hydroxide. The obtained product was dispersed by sonication in ethanol and kept there for further characterization. To prepare the samples for thermal treatment, the suspension solution was dried naturally onto a graphite substrate to form a fragile sheet composed of interweaved products. The samples were examined by scanning probe microscopy (SPM, Digital instrument NS3a controller), SEM (JEOL JSM-6500F at 15 kV) and high-resolution TEM (HRTEM, JEOL JEM-2010). Quantitative analyses were performed by XRD (Mac MXP-18) and Micro-Raman scattering measurements (CHROMEX 501is: 488 nm).

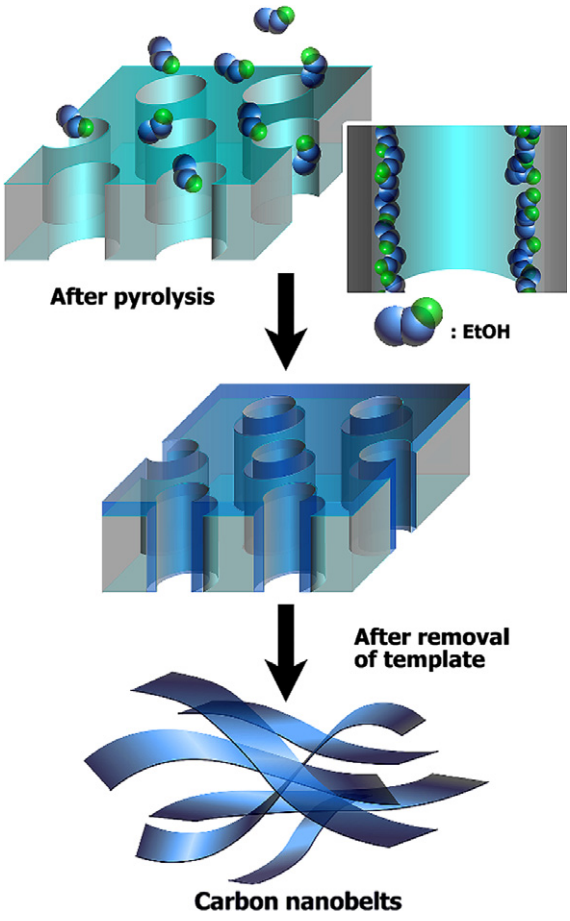

Fig. 1 – The formation of carbon nanobelts with specified sizes.

3. Results and discussion

For study of the morphology and structure, the samples synthesized at 550 °C were dispersed by sonication in ethanol forming a colloidal solution, which was dropped and dried on Si wafer for SEM observation. Fig. 2a shows that the products are in belt-like appearance. The dimensions of the belt-like materials are evaluated to be several to tens of micrometers in length and 470 ± 80 nm in width. Because the channel size of the template is 60 μm in length and 300 ± 50 nm in diameter, therefore it is known that the length of the nanobelt is smaller but the width is larger than the sizes of template channels. The EDS spectrum shows that the products are composed of carbon.

The particle materials underneath a nanobelt can be clearly seen in Fig. 2b. It suggests that the thickness of nanobelts is thin enough to transmit electrons. This phenomenon is also confirmed by the low contrast in TEM image, as shown in Fig. 2c. The inset diffraction pattern in Fig. 2c reveals a pair of blurred diffraction spots which can be assigned to (002) plane of graphite. But the low contrast implies that the crystal domains in as-synthesized materials are localized. The lattice image shown in Fig. 2d was obtained by focusing electron beam on the edge of a 550 °C as-prepared nanobelts. The orientation of graphene layers is roughly parallel to the longitudinal axis of the nanobelts, suggesting that the longitudinal direction is favorable for electron-transport. In this image, the edge region is thick (~ 6.3 nm) enough to observe its lattice clearly, although usually the edge thickness found in our samples is thinner than in this case.

SPM (scanning probe microscopy) image of a segmented nanobelt on the Si substrate is shown in Fig. 3a. In this figure the nanobelt exhibits two convex strips on both edges. The cross-sectional topography plotted in Fig. 3b shows that the height is steep on the edges and becomes flattened in the centre. The result corresponds well with the observation in Fig. 3a. The average thickness in the central part of the nanobelt is 5 nm. The roughness of the background is negligible. The width ratio between the steep regions and the flattened one is evaluated to be 1:2.4:1. And the ratio of length, width, and thickness of the nanobelt is extremely large to be about 1000:100:1 (6 μm:470 nm:5 nm, given by the average values). From the morphological studies, the structure of nanobelt is considered to arise from the collapse of the nanotube, due to the very high ratio between tube diameter and wall thickness. A cross-sectional scheme illustrated in Fig. 3c shows that the thickness of nanobelt should be double of the wall

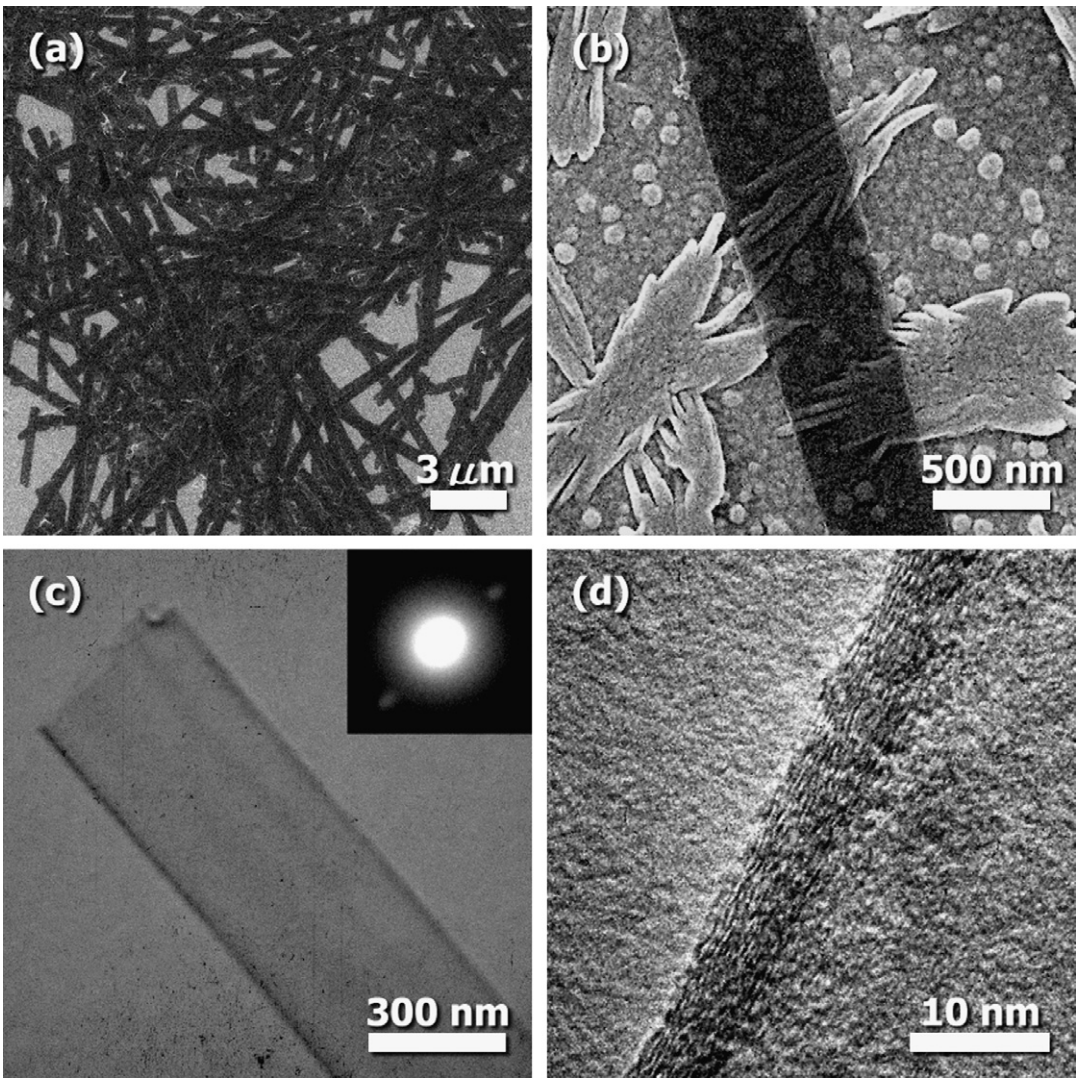

Fig. 2 – (a) Massive amount and (b) a close-up view of the as-synthesized products (550 °C). Bundled products were not found in SEM images. (c) TEM image and (d) lattice image of a nanobelt produced at 550 °C.

thicknesses of collapsed nanotube, and consisted of short-range ordered graphenes as shown in Fig. 2d. According to the great difference among its dimensions, carbon nanobelt can be taken into account in a quasi two-dimensional nanomaterial [12,16].

The formation pathway of our products is proposed: initially carbon from the decomposed ethanol was coated on the surface of cylindrical channels to grow a continuously thin film, which was then collapsed to form belt-like morphology upon the removal of template. Similar results were reported as applying a huge shear stress in multi-walled carbon nanotubes [17]. The radial deformation as a function of the diameter of carbon nanotubes had been discussed earlier [18,19], but the reported aspect-ratio (up to ~21) between tube diameter and wall thickness used in calculation is still much smaller than in our case (~100). It is noticed that there was an experiment carried out by Yu et al., in which the products produced by the decomposition of ethanol into the anodic alumina were carbon nanotubes [20]. The nanotubes were 30 nm in diameter and 5 nm in wall thickness. The ratio of diameter to wall thickness is 6, which is smaller than that of our products (~100), resulting in entirely distinct structures. In addition, various carbon nanobelts can be simply achieved by employing templates with different sizes, as shown in Fig. S1.

Despite the quasi-2D nanobelts have been obtained, the crystallinity of as-synthesized products is poor thus it seems not good enough for developing electronic applications. In order to improve the crystallinity, as-synthesized samples were annealed at 800 °C and 2800 °C, respectively. XRD and Raman data can be found in Fig. 4a and b. There is only one peak exhibited in XRD patterns at $2\theta = 26.5°$, which is assigned to the (002) plane of graphite. The (002) diffraction peak of nanobelts as-synthesized at 550 °C is tiny and cannot be distinguished from the background. After annealing at 800 °C, a small but sharp peak appears. The peak becomes precipitously strong after annealed at 2800 °C. The I_D/I_G ratios estimated from Raman spectra are 1.64 (550 °C as-synthesized sample), 0.57 (800 °C annealed sample), and 0.04 (2800 °C annealed sample), respectively. The I_D/I_G ratio of the sample annealed at 800 °C is lower than that evaluated from

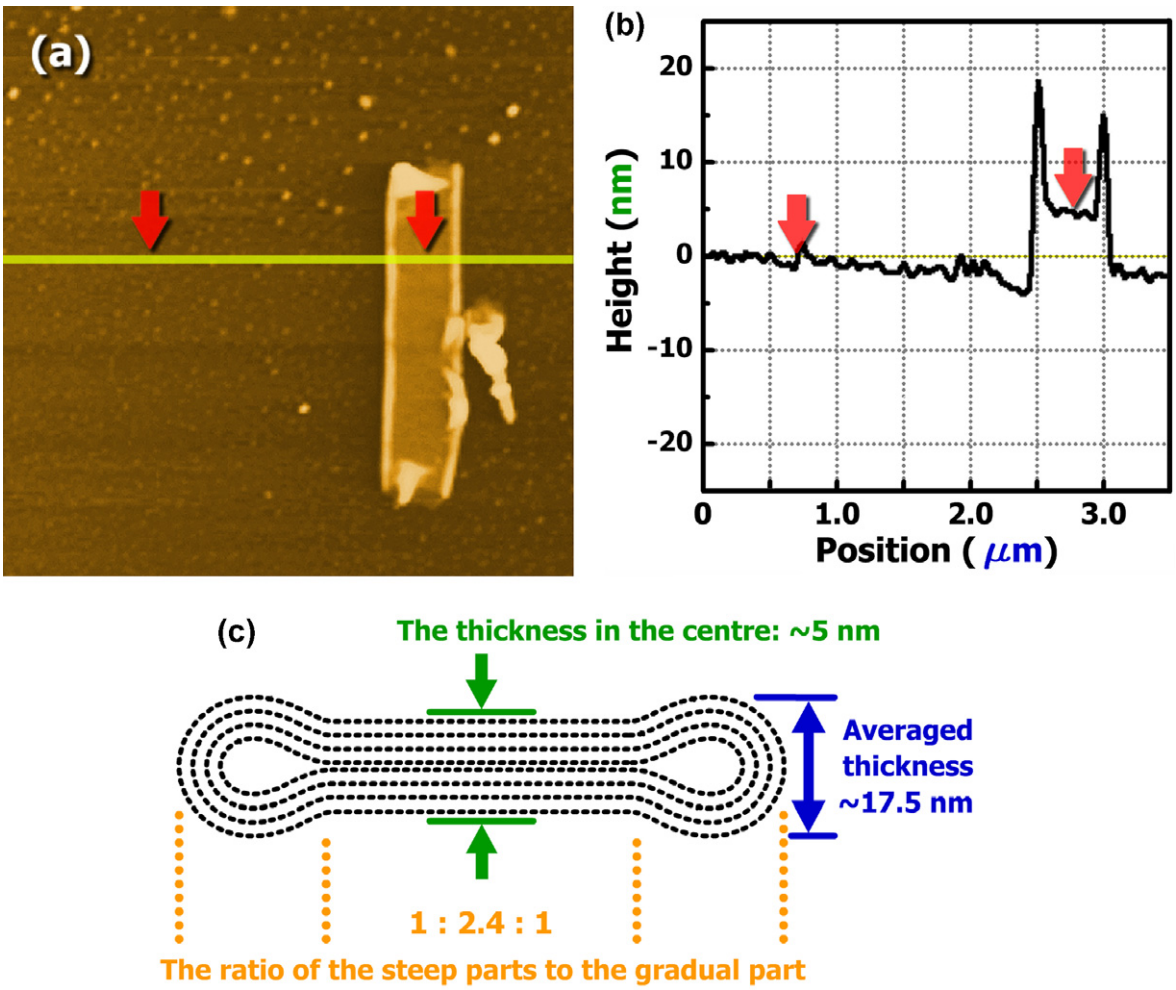

Fig. 3 – (a) The height image and (b) line-scan topography of a segmented nanobelt constructed by scanning probe microscopy. The horizantal lines and the arrows in both figures indicate where the scanning was performed and where the thickness of the sample was estimated, respectively. (c) Cross-sectional illustration of nanobelt shows its sizes and the ratio between them.

conventional multi-walled carbon nanotubes (0.64). The D band vanishes in the spectrum of 2800 °C annealed sample as a result of good crystallinity.

The graphitization of annealed samples was examined under EM observation. As shown in the inset of Fig. 4c, the nanobelt annealed at 800 °C exhibits a pair of obvious (002) diffraction spots, indicating that the crystallinity of 800 °C annealed sample is better than that without treatment. The blurred rings in this figure can be assigned to (100) and (110) planes, which cannot be seen in the inset of Fig. 2c. SEM images of 800 °C annealed nanobelts can be found in Fig. S2. Although the sample annealed at 2800 °C can fulfill even higher graphitization degree, but the belt-like materials will no longer exist. Fig. S3 shows that the nanobelts have merged together after 2800 °C treatment. The results suggest that annealing at 800 °C accomplishes an optimization between quasi-2D structure and crystallinity. A scheme in Fig. 4d illustrates the characteristic morphology of carbon nanobelt.

The nanobelts annealed at 800 °C were then used to investigate the electronic behaviors. The result of the field emission experiment in Fig. 5a shows that the turn-on voltage is 3.25 V/μm. The value is estimated from the Fowler–Nordheim plots, as shown in the inset. The current density is 350 μA/cm^2 at a field of 5.6 V/μm. Even through our samples are not free-standing, the threshold voltage due to the strong edge emitting effect is still lower than that of other quasi-2D nanocarbons [14,21,22]. Long-term stability of our samples was also examined [23], as shown in Fig. 5b. The current efficiency did not obviously decay during 7 h operation, promising the emission stability of nanobelts. The electron pattern and the measurement process in detail are mentioned in Fig. S4.

4. Conclusions

Carbon nanobelts with various sizes could be synthesized by thermal-decomposing ethanol on nanoporous alumina templates. The aspect-ratio of nanobelts is extremely high to be 1000:100:1 (length:width:thickness) and the thickness is only 5 nm. Such morphology can be taken into account in one kind of quasi two-dimensional nanomaterials. The formation

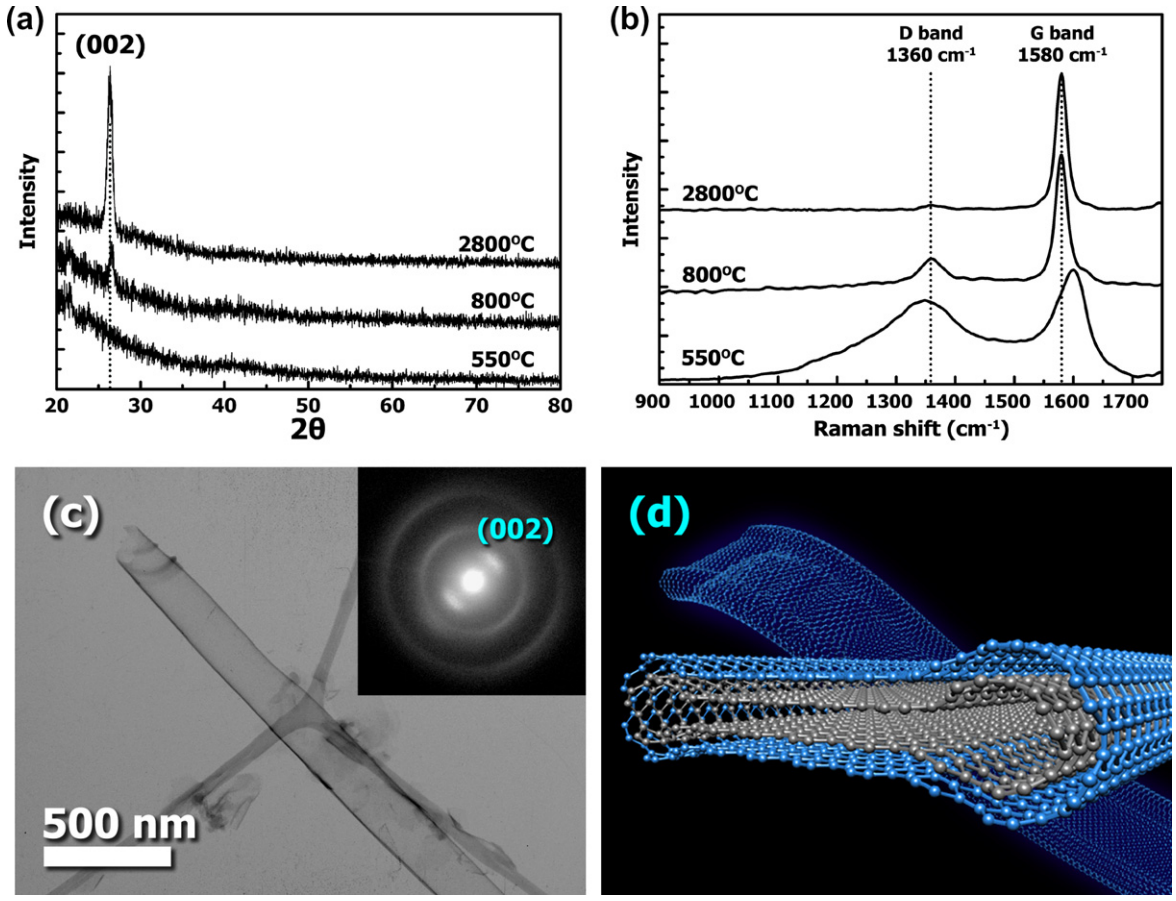

Fig. 4 – (a) XRD and (b) Raman spectra of as-synthesized and annealed nanobelts. The peaks in Raman spectra at 1360 cm^{-1} and 1580 cm^{-1} are assigned to the D band and G band, individually. An arrow points out where the shoulder at 1620 cm^{-1} is shown. (c) TEM image of the carbon nanobelt after annealing at 800 °C. (d) A scheme illustrating the structure of carbon nanobelt.

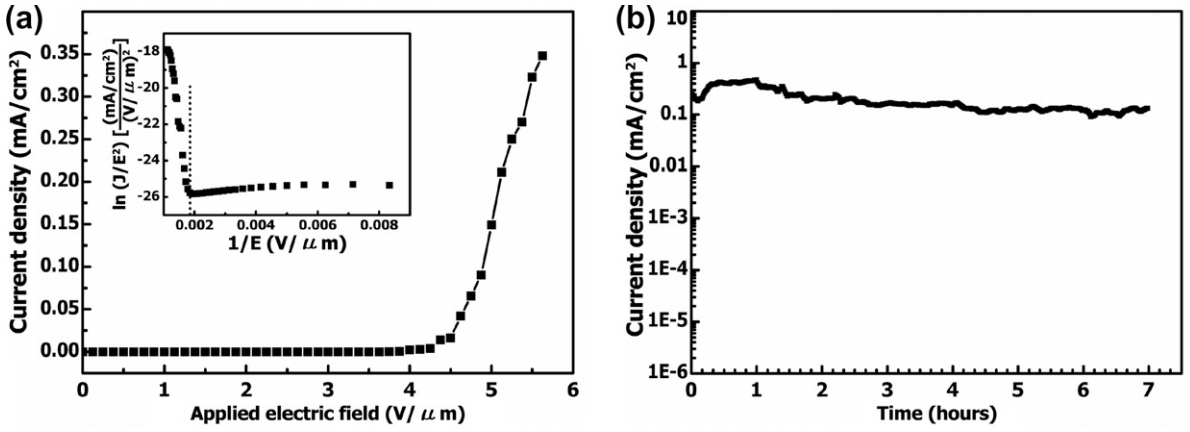

Fig. 5 – (a) The current density (*J*) versus applied electric field (*E*) characteristic and (b) emission stability of the carbon nanobelts which being annealed at 800 °C. The inset in (a) shows the corresponding *F–N* plots.

mechanism was demonstrated to arise from the collapse of nanotube with the large ratio of diameter to wall thickness (>100).

The crystallinity of nanobelts can be improved by thermal treatment, but it needs further investigation to approach toward complete graphene structure. The turn-on voltage obtained from field emitting experiment of the sample annealed at 800 °C is 3.25 V/μm, which is lower than many of current quasi-2D nanocarbons. And long-term emission behavior shows stable efficiency. The high-aspect-ratio

nanomaterial provides a feasible route toward development of nanoelectronics.

Acknowledgements

The authors would like to thank the National Science Council of the Republic of China, Taiwan, for financially supporting this research under Contract Nos. NSC95-2120-M007-008, NSC 94-2213-M-007-035 and NSC 94-2213-M-009-003. Mr. Sun-Ting Yau is acknowledged for the supporting of artwork.

Appendix A. Supplementary data

Supplementary data associated with this article can be found, in the online version, at doi:10.1016/j.carbon.2008.01.034.

REFERENCES

[1] Inagaki M, Kaneko K, Nishizawa T. Nanocarbons – recent research in Japan. Carbon 2004;42(8–9):1401–17.
[2] Kyotani T. Synthesis of various types of nano carbons using the template technique. Bull Chem Soc Jpn 2006;79(9):1322–37.
[3] Lee J, Kim J, Hyeon T. Recent progress in the synthesis of porous carbon materials. Adv Mater 2006;18(16):2073–94.
[4] Zhi L, Wang JJ, Cui GL, Kastler M, Schmaltz B, Kolb U, et al. From well-defined carbon-rich precursors to monodisperse carbon particles with hierarchic structures. Adv Mater 2007;19(14):1849–53.
[5] Kyotani T, Tsai LF, Tomita A. Formation of ultrafine carbon tubes by using an anodic aluminum oxide film as a template. Chem Mater 1995;7(8):1427–8.
[6] Kyotani T, Tsai LF, Tomita A. Preparation of ultrafine carbon tubes in nanochannels of an anodic aluminum oxide film. Chem Mater 1996;8(8):2109–13.
[7] Jian KQ, Shim HS, Schwartzman A, Crawford GP, Hurt RH. Orthogonal carbon nanofibers by template-mediated assembly of discotic mesophase pitch. Adv Mater 2003;15(2):164–7.
[8] Lin CT, Chen WC, Yen MY, Wang LS, Lee CY, Chin TS, et al. Cone-stacked carbon nanofibers with cone angle increasing along the longitudinal axis. Carbon 2007;45(2):411–5.
[9] Kyotani T, Sonobe N, Tomita A. Formation of highly orientated graphite from polyacrylonitrile by using a two-dimensional space between montmorillonite lamellae. Nature 1988;331(6154):331–3.
[10] Kodama M, Nishimura S, Nishikubo K, Kamegawa K, Oshida K. Novel carbon structure prepared using mica as template. Mol Cryst Liquid Cryst 2002;386:217–24.
[11] Lu AH, Schuth F. Nanocasting: a versatile strategy for creating nanostructured porous materials. Adv Mater 2006;18(14):1793–805.
[12] Kang ZH, Wang EB, Mao BD, Su ZM, Lei G, Lian SY, et al. Controllable fabrication of carbon nanotube and nanobelt with a polyoxometalate-assisted mild hydrothermal process. J Am Chem Soc 2005;127(18):6534–5.
[13] Wu YH, Yang BJ, Zong BY, Sun H, Shen ZX, Feng YP. Carbon nanowalls and related materials. J Mater Chem 2004;14(4):469–77.
[14] Wang JJ, Zhu MY, Outlaw RA, Zhao X, Manos DM, Holloway BC, et al. Free-standing subnanometer graphite sheets. Appl Phys Lett 2004;85(7):1265–7.
[15] Masuda H, Fukuda K. Ordered metal nanohole arrays made by a two-step replication of honeycomb structures of anodic alumina. Science 1995;268(5216):1466–8.
[16] Wu YH, Qiao PW, Chong TC, Shen ZX. Carbon nanowalls grown by microwave plasma-enhanced chemical vapor deposition. Adv Mater 2002;14(1):64–7.
[17] Yu MF, Lourie O, Dyer MJ, Moloni K, Kelly TF, Ruoff RS. Strength and breaking mechanism of multi-walled carbon nanotubes under tensile load. Science 2000;287(5453):637–40.
[18] Zhang SL, Khare R, Belytschko T, Hsia KJ, Mielke SL, Schatz GC. Transition states and minimum energy pathways for the collapse of carbon nanotubes. Phys Rev B 2006;73(7):075423. doi:10.1103/PhysRevB.73.075423.
[19] Hasegawa M, Nishidate K. Radial deformation and stability of single-wall carbon nanotubes under hydrostatic pressure. Phys Rev B 2006;74(11):115401. doi:10.1103/PhysRevB.74.115401.
[20] Yu GJ, Wang S, Gong JL, Zhu DZ, He SX, Li YL, et al. Synthesis of carbon nanotube arrays using ethanol in porous anodic aluminum oxide template. Chin Sci Bull 2005;50(11):1097–100.
[21] Shang NG, Au FCK, Meng XM, Lee CS, Bello I, Lee ST. Uniform carbon nanoflake films and their field emissions. Chem Phys Lett 2002;358(3–4):187–91.
[22] Wang SG, Wang JJ, Miraldo P, Zhu MY, Outlaw R, Hou K, et al. High field emission reproducibility and stability of carbon nanosheets and nanosheet-based backgated triode emission devices. Appl Phys Lett 2006;89(18):183103. doi:10.1063/1.2372708.
[23] Lee NS, Chung DS, Han IT, Kang JH, Choi YS, Kim HY, et al. Application of carbon nanotubes to field emission displays. Diam Relat Mater 2001;10(2):265–70.